Coupled fiber taper extraction of 1.53 μm photoluminescence from erbium doped silicon nitride photonic crystal cavities

Gary Shambat[1,*], Yiyang Gong[1], Jesse Lu[1], Selçuk Yerci[2], Rui Li[2], Luca Dal Negro[2], and Jelena Vučković[1]

[1]*Department of Electrical Engineering, Stanford University, Stanford, CA 94305, USA*
[2]*Department of Electrical and Computer Engineering, Boston University, Boston, MA 02215, USA*
**gshambat@stanford.edu*

Abstract: Optical fiber tapers are used to collect photoluminescence emission at ~1.5 μm from photonic crystal cavities fabricated in erbium doped silicon nitride on silicon. In the experiment, photoluminescence collection via one arm of the fiber taper is enhanced 2.5 times relative to free space collection, corresponding to a net collection efficiency of 4%. Theoretically, the collection efficiency into one arm of the fiber-taper with this material system and cavity design can be as high as 12.5%, but the degradation of the experimental coupling efficiency relative to this value mainly comes from scattering loss within the short taper transition regions. By varying the fiber taper offset from the cavity, a broad tuning range of coupling strength and collection efficiency is obtained. This material system combined with fiber taper collection is promising for building on-chip optical amplifiers.

OCIS codes: (230.5298) Photonic crystals; (230.5750) Resonators; (130.3120) Integrated optics devices; (060.2310) Fiber optics and optical communications: Fiber optics

References and links

1. D. A. B. Miller, "Device requirements for optical interconnects to silicon chips," Proc. IEEE **97**(7), 1166–1185 (2009).
2. L. Liao, A. Liu, D. Rubin, J. Basak, Y. Chetrit, H. Nguyen, R. Cohen, N. Izhaky, and M. Paniccia, "40 Gbit/s silicon optical modulator for high speed applications," Electron. Lett. **43**(22), 1196–1197 (2007).
3. P. Dong, S. Liao, D. Feng, H. Liang, D. Zheng, R. Shafiiha, C. C. Kung, W. Qian, G. Li, X. Zheng, A. V. Krishnamoorthy, and M. Asghari, "Low V_{pp}, ultralow-energy, compact, high-speed silicon electro-optic modulator," Opt. Express **17**(25), 22484–22490 (2009).
4. L. Colace, M. Balbi, G. Masini, G. Assanto, H. C. Luan, and L. C. Kimerling, "Ge on Si p-i-n photodiodes operating at 10 Gb/s," Appl. Phys. Lett. **88**(10), 101111 (2006).
5. O. Fidaner, A. K. Okyay, J. E. Roth, R. K. Schaevitz, Y.-H. Kuo, K. C. Saraswat, J. S. Harris, Jr., and D. A. B. Miller, "Ge-SiGe quantum-well waveguide photodetectors on silicon for the near-infrared," IEEE Photon. Technol. Lett. **19**(20), 1631–1633 (2007).
6. M. Makarova, Y. Gong, S.-L. Cheng, Y. Nishi, S. Yerci, R. Li, L. Dal Negro, and J. Vuckovic, "Photonic crystal and plasmonic silicon based light sources," IEEE J. Sel. Top. Quantum Electron. **16**(1), 132–139 (2010).
7. Y. Gong, M. Makarova, S. Yerci, R. Li, M. J. Stevens, B. Baek, S. W. Nam, R. H. Hadfield, S. N. Dorenbos, V. Zwiller, J. Vuckovic, and L. Dal Negro, "Linewidth narrowing and Purcell enhancement in photonic crystal cavities on an Er-doped silicon nitride platform," Opt. Express **18**(3), 2601–2612 (2010).
8. K. Srinivasan, P. E. Barclay, M. Borselli, and O. J. Painter, "An optical-fiber-based probe for photonic crystal microcavities," IEEE J. Sel. Areas Comm. **23**(7), 1321–1329 (2005).
9. C. Grillet, C. Monat, C. Smith, B. Eggleton, D. Moss, S. Frederick, D. Dalacu, P. Poole, J. Lapointe, G. Aers, and R. Williams, "Nanowire coupling to photonic crystal nanocavities for single photon sources," Opt. Express **15**(3),1267 (2007).
10. I. Hwang, S. K. Kim, J. Yang, S. H. Kim, S. Lee, and Y. Lee, "Curved-microfiber photon coupling for photonic crystal light emitter," Appl. Phys. Lett. **87**(13), 131107 (2005).
11. T. A. Birks, and Y. W. Li, "The Shape of Fiber Tapers," J. Lightwave Technol. **10**(4), 432–438 (1992).
12. Y. Jung, G. Brambilla, and D. J. Richardson, "Optical microfiber coupler for broadband single-mode operation," Opt. Express **17**(7), 5273–5278 (2009).
13. S. Yerci, R. Li, O. Kucheyev, T. van Buuren, S. Basu, and L. Dal Negro, "Energy transfer and 1.54 μm emission in amorphous silicon nitride films," Appl. Phys. Lett. **95**(3), 031107 (2009).

#122219 - $15.00 USD Received 4 Jan 2010; revised 25 Feb 2010; accepted 1 Mar 2010; published 10 Mar 2010

14. Y. Akahane, T. Asano, B. S. Song, and S. Noda, "High-Q photonic nanocavity in a two-dimensional photonic crystal," Nature **425**(6961), 944–947 (2003).
15. J. Vuckovic, M. Loncar, H. Mabuchi, and A. Scherer, "Optimization of the Q factor in photonic crystal microcavities," IEEE J. Quantum Electron. **38**(7), 850–856 (2002).
16. M. Kim, J. Yang, Y. Lee, and I. Hwang, "Influence of etching slope on two-dimensional photonic crystal slab resonators," J Korean Phys Soc. **50**(4), 1027–1031 (2007).
17. S. Iwamoto, Y. Arakawa, and A. Gomyo, "Observation of enhanced photoluminescence from silicon photonic crystal nanocavity at room temperature," Appl. Phys. Lett. **91**(21), 211104 (2007).
18. C. Manolatou, M. J. Khan, S. Fan, P. R. Villeneuve, H. A. Haus, and J. D. Joannopoulos, "Coupling of modes analysis of resonant channel add–drop filters," IEEE J. Quantum Electron. **35**(9), 1322–1331 (1999).
19. I. Hwang, G. Kim, and Y. Lee, "Optimization of coupling between photonic crystal resonator and curved microfiber," IEEE J. Quantum Electron. **42**(2), 131–136 (2006).
20. M. W. Lee, C. Grillet, C. G. Poulton, C. Monat, C. L. C. Smith, E. Mägi, D. Freeman, S. Madden, B. Luther-Davies, and B. J. Eggleton, "Characterizing photonic crystal waveguides with an expanded k-space evanescent coupling technique," Opt. Express **16**(18), 13800–13808 (2008).
21. I. Hwang, and Y. Lee, "Unidirectional, efficiency-controlled coupling from microcavity using reflection feedback," IEEE J. Sel. Top. Quantum Electron. **13**(2), 209–213 (2007).

1. Introduction

Optical interconnects have the potential to improve data communication in computer systems by providing a high bandwidth, low power alternative to present electrical interconnects. Particularly for off-chip links, where traditional metal interconnects suffer from large capacitive delays and high energy consumption, implementing optical interconnects may be very advantageous [1]. While much progress has been made with CMOS-compatible modulators and detectors [2–5], a suitable light source that is well integrated with a silicon platform remains to be demonstrated. Due to silicon's indirect band gap, light emission from the semiconductor is weak and alternatives methods of light extraction such as through incorporated emitters are necessary. Recently, it was shown that photonic crystal (PC) cavities in erbium-doped silicon nitride ($Er:SiN_x$) exhibited linewidth narrowing with increased optical pump power [6,7], demonstrating that 31% of Er ions can be excited under optical pumping. The amorphous silicon nitride provides a host for erbium dopants which luminesce at the traditional telecom wavelength range. Such a material may be suitable for an on-chip amplifier or laser source in the future.

To connect a nanoscale photonic crystal cavity to the off-chip environment of an optical interconnect system, silica fiber tapers may be used to in- and out-couple light efficiently. Fiber tapers have been shown to be useful not only in probing and characterizing cavities [8,9], but also in providing optical pumping for a laser and extracting photoluminescence [10]. Because fiber tapers rely on resonant evanescent coupling, they can inject and extract light with much higher efficiency than with free space techniques. We report the first study on the extraction of photoluminescence from $Er:SiN_x$ PC cavities using fiber tapers. We find that a greater collection efficiency can be obtained using the evanescent coupling method compared to out-coupling through free space; experimentally, the collection efficiency into a single arm of the fiber taper is increased 2.5 times relative to free space, and theoretically this could be improved by another factor of 3 by minimizing the scattering losses within the short taper transition regions. We also demonstrate that a broad tuning range of quality factor (up to 98% of the intrinsic Q value) is attainable by altering the strength of the coupling and thus the coupling efficiency.

2. Fabrication

2.1 Taper fabrication

Fiber tapers were fabricated using the well known "flame brushing" technique [11] in which a standard single mode communication fiber is simultaneously heated by a torch and pulled outward by motorized stages. A hydrogen-oxygen torch was used to provide a small flame that was quickly scanned back and forth along the designated "hot zone" of the fiber. In order to provide the best mechanical stability of the taper probe, the pull length was kept to only ~3 mm, while the taper diameter was ~1 μm. This diameter was chosen because when the taper is below approximately 1.1 μm the waveguide becomes single mode [12]. This single

#122219 - $15.00 USD Received 4 Jan 2010; revised 25 Feb 2010; accepted 1 Mar 2010; published 10 Mar 2010

mode behavior cleans up coupling spectra and removes erroneous fringing in the transmission and photoluminescence spectra. After the fiber tapers were drawn, they were carefully bent such that the radius of curvature was small enough for the tapers to interact only with photonic crystal cavities and not the nearby substrate. An optical image of a fabricated taper is shown in Fig. 1(a). The whole fiber was mounted to a glass slide and was fusion spliced into connector cables. Finally, the slide was mounted in a measurement rig where the taper could be positioned onto photonic crystal cavities via both motorized and manual nanopositioning stages. The transmission of the mounted fiber taper was 16%, with most of the loss coming from scattering within the short taper transition regions.

2.2 Cavity fabrication

Photonic crystal structures were fabricated in a two layer membrane consisting of a bottom silicon layer and a top, light emitting, erbium-doped silicon nitride (Er:SiNx) layer, same as in our previous work [7]. Approximately 110 nm of erbium-doped amorphous silicon nitride was deposited on a silicon on insulator (SOI) wafer with a silicon thickness of 250 nm by N_2 reactive magnetron co-sputtering from Si and Er targets in a Denton Discovery 18 confocal-target sputtering system [13].

Photonic crystal L3 cavities [14] were patterned with an electron beam lithography system using ZEP-520A as the resist. A Cl_2:HBr dry etch chemistry was used to etch the air holes and the sacrificial oxide layer in the SOI was undercut at the end using a 6:1 Buffered oxide etch to form the suspended PC membrane. The lattice periodicity was set to a = 410 nm, and hole radius was r = 125 nm. Additional outward shifts of 0.15a and 0.075a for the on-axis holes surrounding the cavity were made to increase the intrinsic Q of the cavity. Figure 1(b) shows a scanning electron microscope (SEM) image of the tested cavity.

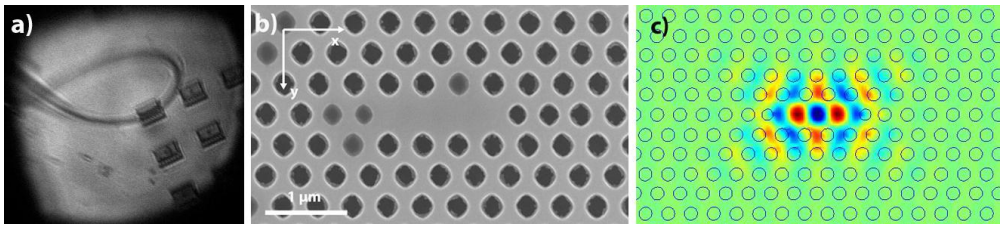

Fig. 1. (a) Optical microscope image of the fiber taper. (b) SEM picture of the fabricated SiN_x/Si photonic crystal cavity. (c) Calculated E_y field of the fundamental mode of the photonic crystal.

3. Theoretical analysis

3.1 – Free space collection efficiency

Finite difference time domain (FDTD) calculations were performed on the cavity structure with the size parameters of the SEM image above. The computational grid contained 10 mirror periods on each side of the cavity in the y direction and 12 mirror periods on each side in the x direction. Q-factor calculations were performed by integrating the power flux through the appropriate boundaries: top and bottom half spaces for the vertical Q's, slab walls for the in-plane Q, and fiber facets for the fiber Q. The fundamental mode profile is shown in Fig. 1(c).

In order to estimate the percentage of light collected by our microscope objective (in free space collection), a far-field calculation of the cavity mode was performed using a two-dimensional Fourier Transform to calculate its k-space distribution [15]. This method allows for the accurate prediction of power flow through a particular geometrical cone of radiation without requiring a massive FDTD space. In the limit that the full hemisphere of radiation is chosen, the vertical Q would be recovered, in agreement with FDTD simulations. For this study, the total power radiated within a 0.5 numerical aperture (NA) objective was determined to be 10% of the total emission into the half space above the slab. The low value is not

#122219 - $15.00 USD Received 4 Jan 2010; revised 25 Feb 2010; accepted 1 Mar 2010; published 10 Mar 2010

surprising if one examines the k-space map for the cavity E_y field shown in Fig. 2. The transverse electric-like (TE-like) fundamental mode is predominantly E_y in character and from the k-space pattern in Fig. 2(b), we see that the magnitude of the components radiated within the NA cone is much smaller than the sum inside the light cone. By taking account radiation through the slab and bottom direction, the total efficiency of collection into the objective is given as $0.1 \cdot 1/Q_{top}/(1/Q_{top} + 1/Q_{||} + 1/Q_{bot}) = 1.6\%$, where Q_{top}, $Q_{||}$, and Q_{bot} denote the top, in-plane, and bottom Q's, respectively.

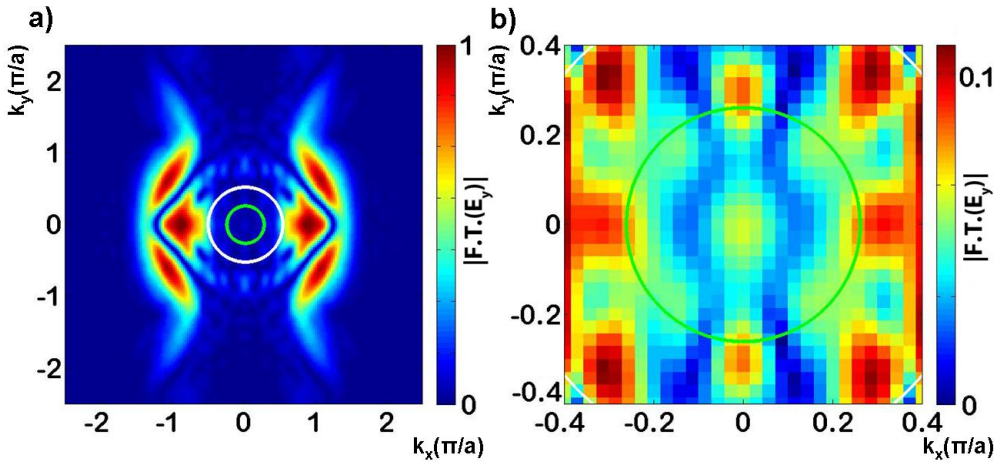

Fig. 2. (a) K-space map for the E_y component of the fundamental mode, taken just above the PC slab. The white circle is the light cone while the green circle is the NA = 0.5 cone. (b) Zoomed in image of the previous plot highlighting the difference between the radiated components captured and not captured by the objective lens. The magnitude of the k components inside the NA = 0.5 cone is clearly much lower than those outside the cone.

3.2 – Coupled cavity Q-factor

The intrinsic cavity Q for the fundamental mode was found to be 16,000 and is dominated by the in-plane Q which was only 26,000. Due to asymmetry of the PC in the vertical direction, the confined TE-like cavity mode couples to TM-like propagating Bloch states, which suffer from an incomplete bandgap and hence leak out of the cavity [16]. In contrast, a similar PC structure composed of just the symmetric silicon layer has an in-plane Q of nearly 900,000 and a net Q of 61,000.

Figure 3 shows a plot of the various Q-factors as a fiber taper, represented as a cylinder of silica (n = 1.45, diameter = 1 μm), is scanned across the surface of the L3 cavity along the y-axis. For zero offset, we see that the fiber Q (Q_f) is low, indicating a high decay rate due to the evanescent coupling into the fiber. (We note that Q_f describes the power coupled from the cavity to the fiber taper, and is calculated by integrating power lost through both ends of the fiber taper). The cavity in-plane Q ($Q_{||}$) is also reduced by a factor of two due to the increased vertical asymmetry of the structure. This parasitic decay reduces the total Q (Q_{tot}) beyond the intrinsic limit of just additional decay into the fiber.

As the taper is shifted to the side of the cavity, several trends can be observed. First, Q_f remains relatively constant up to 350 nm before increasing exponentially with taper offset. The decrease in coupling strength due to a smaller evanescent field overlap for the offset taper causes Q_f to increase exponentially. Second, there are points of enhanced parasitic loss at 350 nm and 1 μm as is evidenced by the reduction in $Q_{||}$ and Q_{tot}. These points are likely regions where the composite cavity structure has greatest asymmetry and coupling into leaky TM modes. Finally, as the taper displacement grows beyond 1.2 μm, all Q values asymptotically approach their intrinsic limits. We still see that even for large offsets, the fiber taper can couple with the cavity without inducing parasitic decay. In particular, at 1.2 μm offset, $Q_{||}$ is

#122219 - $15.00 USD Received 4 Jan 2010; revised 25 Feb 2010; accepted 1 Mar 2010; published 10 Mar 2010

close to its intrinsic limit and the coupling efficiency is given by $\eta = (1/Q_f)/(1/Q_{tot}) = 13{,}000/553{,}000 = 2.4\%$. The maximal coupling strength is expectedly seen to occur when the taper offset is zero. In this case, the coupling efficiency is 25%. Therefore simulations predict that a much larger (~16-fold) coupling efficiency can be achieved into the fiber relative to the coupling to free space and a collection lens of NA = 0.5.

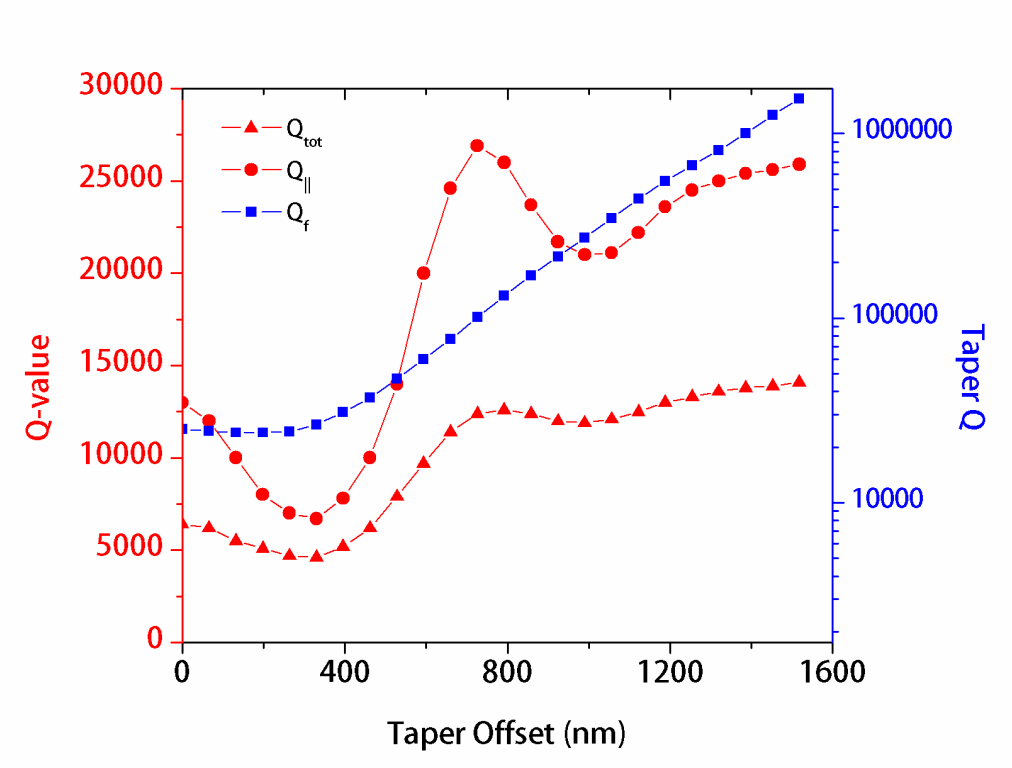

Fig. 3. Variation of the fiber, in-plane, and total Q factors as a function of taper displacement, d, along the y axis. When the taper is directly over the cavity, the fiber Q goes down expectedly and the in-plane Q is parasitically reduced by a factor of two. For large taper offsets, the Q-values approach their intrinsic limits. Inset shows the cross-section of the FDTD simulated structure. The taper is aligned along the cavity axis direction (i.e., the x direction in Fig. 1) and is displaced along the y direction.

4. Experiment

4.1 – Free space photoluminescence

Photoluminescence (PL) from fabricated photonic crystal cavities was collected in free space, in the direction perpendicular to the PC plane, through a 100x (NA = 0.5) objective lens, directed toward a monochromator, and detected with a liquid nitrogen cooled linear InGaAs CCD array, same as in our earlier work [7]. PL from the cavity region was spatially filtered with an iris in order to minimize the background signal and optimized for greatest collection efficiency. Samples were pumped with a 980 nm laser diode at 6 mW measured before the objective lens. Figure 4 displays the PL of the L3 cavity showing the fundamental resonance at approximately 1535.2 nm at the maximum of erbium's typical emission spectrum. This particular cavity was chosen for testing because its cavity resonance overlaps with the peak emission of erbium. A higher order mode is observed at 1480 nm and the features at 1560 nm are likely band edge modes [17]. The measured Q value of the intrinsic, unloaded cavity was found to be 12,630 as seen by the fit to a Lorentzian in the inset of Fig. 4.

#122219 - $15.00 USD Received 4 Jan 2010; revised 25 Feb 2010; accepted 1 Mar 2010; published 10 Mar 2010

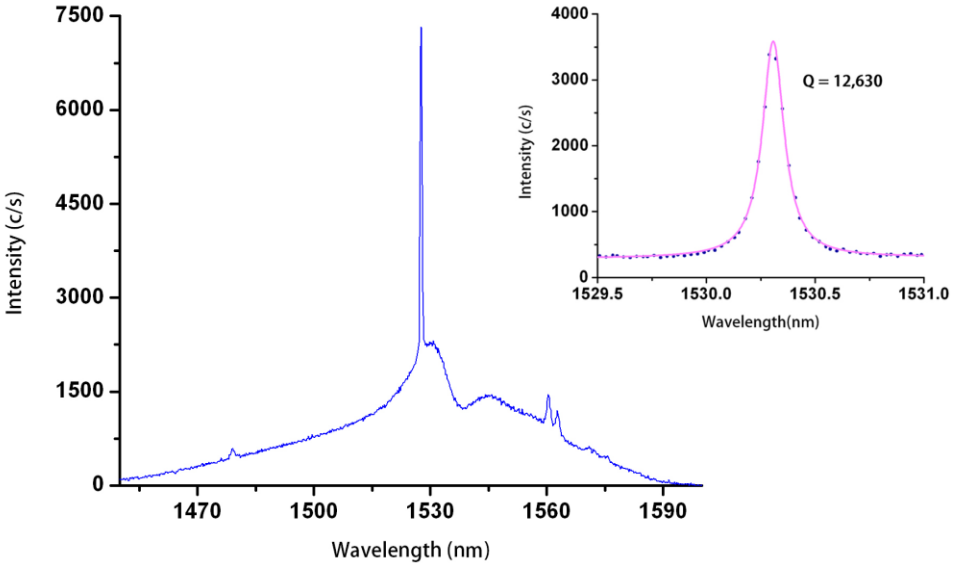

Fig. 4. PL spectrum of the Er:SiNx on Si PC cavity, collected from free space in the direction perpendicular to the PC plane (through an objective lens with NA = 0.5). The fundamental cavity mode corresponds to the highest peak near 1530nm, and the background emission has the expected erbium profile. The inset shows the fundamental peak zoomed in with a Lorentzian fit.

4.2 – Passive (transmission) cavity measurements via fiber taper

Transmission measurements were performed by coupling a broadband source into a fiber taper that was well aligned with an L3 cavity main axis, and by measuring the spectrum at the output of the fiber with an optical spectrum analyzer (OSA) (Fig. 5(a)). Light was not polarized at the input so that all the modes of the cavity could be excited, thus facilitating the identification of the fundamental mode. The taper rested on the sample surface.

Figure 5(b) shows a full transmission spectrum of the cavity whose PL is shown in Fig. 4. The fundamental resonance is clearly seen at about 1530 nm, as in Fig. 4, as well as two higher order modes at shorter wavelengths. Four additional modes were found at wavelengths below 1400 nm. The background loss of 2-5 dB comes primarily from TM loss in the PC slab.

#122219 - $15.00 USD Received 4 Jan 2010; revised 25 Feb 2010; accepted 1 Mar 2010; published 10 Mar 2010

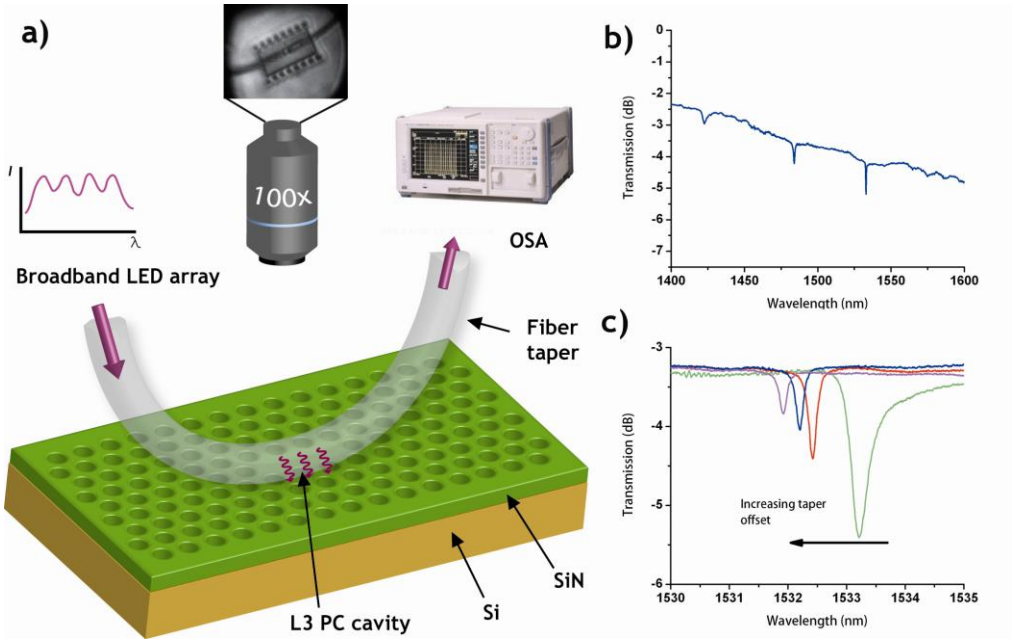

Fig. 5. (a) Experimental setup for measurement of transmission through the Er:SiNx on Si PC cavities via fiber taper. The fiber taper is aligned and in contact with the L3 cavity. The output spectrum of a broadband source at the input of the fiber is measured by an OSA. Inset shows optical picture of aligned taper. (b) Full transmission spectrum of the L3 cavity. (c) Multiple transmission spectra for the same cavity but with different fiber taper offsets along the y axis.

In Fig. 5(c), multiple transmission scans are taken for the taper as it is progressively offset from the main axis in of the cavity in the y-direction. The short pull length of the taper was necessary for the tension of the fiber to be large enough to allow this seamless translation, which is otherwise prevented by the Van der Waals sticking attraction between the fiber and semiconductor. As can be seen in the plot, as the fiber taper is dragged away from the cavity center, the transmission coupling magnitude drops and the Q factor increases. This is not surprising since the coupling coefficient is given by the overlap between the cavity and waveguide modes [18]. As the taper shifts, this overlap decreases along with the transmission coupling. Likewise, since this secondary decay path via the taper decreases with taper offset, the measured Q value approaches the intrinsic limit. Also worth noting is the red shift induced by the taper as it moves over the cavity which is due to the increased effective index of the cavity.

4.3 – Fiber-outcoupled photoluminescence

Fiber taper coupling provides a convenient means to extract and collect photoluminescence from a cavity mode that would ordinarily radiate non-uniformly into free space. A well designed cavity (such as the described L3 type) is meant to have few wave vector components in the light cone in order to maximize the Q (see Fig. 2) [14]. The fiber taper can, on the other hand, extract those components that are outside the light cone through evanescent coupling.

PL measurements with a coupled fiber taper were taken under similar conditions as those for the free space measurement. To do so, a 980 nm laser diode pump with power 6 mW was focused to a small spot where the fiber taper rested on the cavity. The output from one end of the fiber was then sent to the same spectrometer setup as before (Fig. 6(a)).

#122219 - $15.00 USD Received 4 Jan 2010; revised 25 Feb 2010; accepted 1 Mar 2010; published 10 Mar 2010

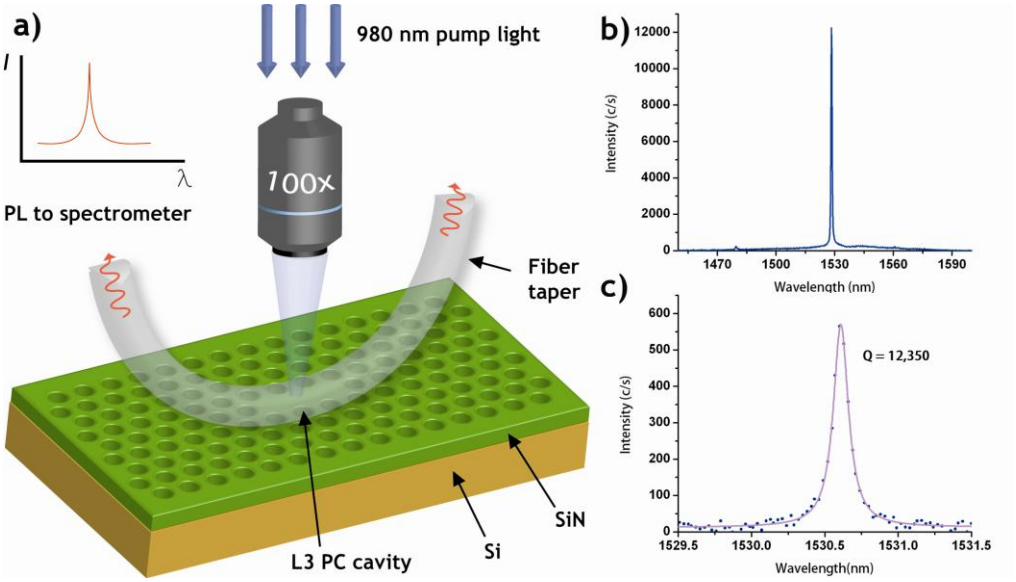

Fig. 6. (a) Experimental setup for outcoupling PL from Er:SiNx on Si PC cavities via fiber tapers. Pump light is focused on the cavity while PL emission is collected by the same fiber taper and sent to a spectrometer. (b) Full PL spectrum for fiber-coupled emission from the PC cavity. The integrated intensity is 2.5x larger than for the free space measurement and the peak has a Q of 4,300. (c) A different data point for which the taper was offset from the cavity so that the cavity was minimally loaded.

When the taper is positioned over the center of the cavity, the PL extraction is maximized as can be seen in Fig. 6(b). The non-resonant background PL of erbium is minimized in this configuration while the integrated intensity of the fundamental mode is 2.5 times that collected through free space (in the vertical direction) and an NA = 0.5 objective lens (Fig. 4). Since the taper has a total transmission of ~0.16, the transmission of each taper arm is roughly 0.4 assuming symmetric loss. This means that the PL intensity coupled into one taper arm before loss is actually 2.5/0.4 = 6.25 times the free space collected PL. Adding the contribution from both taper arms gives a total enhancement of 12.5 before loss. Since the radiation calculation revealed that collection through free space is 1.6%, the total fiber coupling efficiency is 20%, while the total fiber collection efficiency through one arm with loss is 4%. This lossless efficiency value is pretty close to the result predicted by simulation and the slight discrepancy could be due to differences in the actual taper size and exact taper positioning. Such a high extraction efficiency is made possible because the fiber taper relies on evanescent coupling from the cavity and is not limited geometrically by the finite extent of an objective lens. It is interesting to note that a large coupling ratio can be obtained despite the phase matching between the taper and cavity not being fully optimized [19]. This is a result of the fact that a strongly localized cavity resonance spans a number of k-vectors, which permits coupling to a taper mode. Additionally, the curved taper itself spans a wide k-space [20] as was found out from separate coupling experiments with waveguides.

Figure 6(c) shows the PL of the cavity resonance for the case when the taper is displaced from the cavity main axis. The Q in this case is found to be approximately 12,350, which corresponds to 98% of the intrinsic Q value. Coupling to fiber tapers in direct contact measurements is usually associated with high loading of the cavities due to either direct coupling into the fiber or parasitic loss into other decay paths [19]. As expected, we confirm that by reducing the coupling strength (by decreasing the mode field overlap), the cavity Q can remain very high. This agrees with simulation results in Fig. 3. The ability to have a control over the cavity Q is important for PC cavity-based lasers or amplifiers which need to have as low loss as possible.

#122219 - $15.00 USD Received 4 Jan 2010; revised 25 Feb 2010; accepted 1 Mar 2010; published 10 Mar 2010

To more clearly see the relationship between collection efficiency and measured Q value, a series of spectra were taken for various taper offsets from the cavity as seen in Fig. 7(a). The fiber taper was slowly displaced along y-direction and as expected, the measured cavity Q increased while the collected intensity decreased. Figure 7(b) shows a few traces at different coupling strengths where the intensity-Q relationship is seen clearly. This behavior can be described by an efficiency relationship under the condition that no parasitic loading of the cavity takes place [9]:

$$\eta = 1 - \frac{Q_t}{Q_0} \tag{1}$$

Here η is the collection efficiency given as the decay rate into the fiber divided by the total decay rate, Q_t is the loaded cavity Q, and Q_0 is the intrinsic Q. The straight line in Fig. 7(a) is a fit to the data using Eq. (1). As can be seen in the plot, the fit is only good for the region of low coupling (high Q) and deviates significantly where taper loading is strong. This is expected from simulations, since for high coupling the parasitic loss grows and the denominator in Eq. (1) would have to be modified by adding the parasitic loss, and thereby lowering the intrinsic Q_0 value. The additional degradation is due to the newly generated decay from the parasitic TM coupling. For example, the data point with Q = 4,300 and collected intensity 43,000 counts per second (corresponding to Fig. 6(b) above) should have an efficiency of η = 1 – 4,300/12,630 = 0.66. However, the actual efficiency is limited to 0.2 due to the parasitic loss which reduces Q_0.

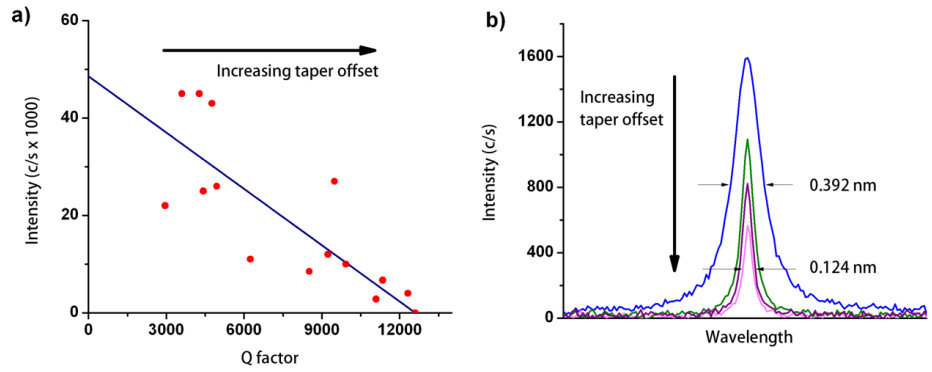

Fig. 7. (a) Collected PL intensity and the total cavity Q-factor as the fiber taper is offset from the cavity along the y-direction. The blue line is a fit to the data. (b) Several spectra for the data in (a). As the taper moves away from the cavity the integrated intensity decreases and the Q increases. The peaks are centered together for easier visualization (but as shown in Fig. 6, the cavity resonance redshifts for higher cavity-taper overlap).

5. Conclusion

In summary, we demonstrate fiber taper coupling and efficient PL extraction from a CMOS-compatible light-emitting material, Er:SiNx embedded in a Si PC cavity. The collection efficiency through one arm of the fiber taper was 2.5 times the collection through free space and an objective lens with NA = 0.5. Better fabrication of short tapers or using long lossless tapers coupled to cavities on elevated membranes [8] could improve the collection efficiency into one taper arm by another factor of 3. Finally, the full collection enhancement of 12.5 times could be achieved with an interferometric taper design where the full signal is collected into one arm [21]. Larger collection enhancements are also possible by better phase matching of the fiber and cavity modes. The loaded quality factor of the coupled cavity can remain very high and in the limit of weak coupling can be as high as 98% of its intrinsic value. A broad

#122219 - $15.00 USD Received 4 Jan 2010; revised 25 Feb 2010; accepted 1 Mar 2010; published 10 Mar 2010

tuning range of collection efficiencies and quality factors is made possible by a variable coupling strength inversely proportional to the taper displacement from the cavity. The fiber taper provides a convenient platform for linking the nano-scale on-chip environment with the off-chip interconnect network, which is important for building devices such as on-chip optical amplifiers. For the promising erbium-doped silicon nitride material, fiber coupled emission is an easy and efficient way to extract light and connect to outside systems.

Acknowledgements

The authors would like to acknowledge the MARCO Interconnect Focus Center and the U.S. Air Force MURI program under Award No. FA9550-06-1-0470 for funding. Gary Shambat and Yiyang Gong would also like to thank the NSF GRF for support. The fabrication has been performed in the Stanford Nanofabrication Facilities.

#122219 - $15.00 USD Received 4 Jan 2010; revised 25 Feb 2010; accepted 1 Mar 2010; published 10 Mar 2010